

# Observation of relaxation resonance effects in the field spectrum of semiconductor lasers

K. Vahala, Ch. Harder, and A. Yariv  
*California Institute of Technology 128-95, Pasadena, California 91125*

(Received 7 September 1982; accepted for publication 9 November 1982)

Subsidiary maxima are observed in the field spectra of single mode semiconductor lasers. Measurements of their power dependence show they are linked to the relaxation resonance. We attribute these maxima to combined phase and amplitude fluctuations at the relaxation resonance. A theoretical calculation of the field spectrum using the results of a noise analysis incorporating carrier dynamics agrees very well with observations.

PACS numbers: 42.55.Px, 42.60.Fc, 42.60.Kg

As applications of semiconductor lasers have become more widespread interest has increased in characterizing their noise properties. Their extremely high gain as well as strong amplitude-phase coupling causes their noise spectra to differ markedly from other laser systems. Vahala and Yariv<sup>1</sup> have recently done a theoretical analysis of the fundamental noise properties of semiconductor lasers which includes the carrier density as a dynamical variable and the carrier density dependence of the refractive index. Standard treatments on semiconductor laser noise<sup>2</sup> model the laser as a first order system and predict that its field spectrum is Lorentzian. When carrier dynamics are included, however, the model is second order and accounts for effects such as the relaxation resonance. As a consequence the laser field spectrum predicted by the second order model is not an exact Lorentzian. Instead, the field spectrum consists of the main lasing line surrounded by subsidiary maxima (side bands) spaced at intervals of the relaxation resonant frequency. These sidebands have been observed in certain semiconductor lasers,<sup>3</sup> but were not explained completely. Until now there is no experimental evidence that shows they are linked to the relaxation resonance. We have observed field spectrum sidebands and in this letter present data which shows they are a consequence of the relaxation resonance. Using the theoretical results of Vahala and Yariv we also show that asymmetry in the sidebands gives a measure of the correlation between amplitude and phase fluctuations.

Hitachi HLP3400 buried optical guide (BOG) and HLP1400 channeled substrate planar (CSP) GaAlAs lasers with threshold currents of 20 and 57 mA at room temperature were measured. The bias current to the lasers was passed through a low pass filter. To prevent instabilities caused by optical feedback a neutral density filter (ND5) was inserted at an angle between the test laser and a microscope objective which collimated the beam into a scanning Fabry-Perot interferometer. The severely attenuated output signal was detected using a photomultiplier. Both lasers exhibited fundamental inverse power field linewidth broadening when measured using a scanning Fabry-Perot interferometer with a 1500-MHz free-spectral range and an instrumental bandwidth of approximately 12 MHz. Predominately single mode operation was achieved for bias points a few milliamperes above threshold, other modes being two to three orders smaller than the lasing mode. The field spectrum sidebands

were measured using a monochromator in tandem with a scanning Fabry-Perot with a free-spectral range of 7.5 GHz and an instrumental bandwidth of 70 MHz. The monochromator served as a wide bandpass, preventing weakly excited longitudinal modes from obscuring observations. Scan rates were adjusted so that any distortion caused by detection time constants was not noticeable. The output of the photomultiplier drove the y axis of an oscilloscope whose sweep was synchronized to the Fabry-Perot interferometer.

Figure 1 is a typical output which shows the lasing line shape twice. This photograph was taken using the CSP biased at 66 mA, which corresponds to 16% above threshold and an optical output power of 2.0 mW. The vertical magnification is  $100\times$  that normally used for viewing the field spectrum. This has caused the center lobe to be clipped. The first order sidebands are clearly visible and are separated from line center by 1.7 GHz. The sideband amplitude at this bias point is roughly 1% of the lasing peak amplitude and its absolute strength was observed to decrease with increasing power. Sidebands observed on the BOG exhibited the same amplitude power dependence, but their relative size was an order of magnitude smaller than those observed on the CSP. Higher order sideband amplitudes have been calculated using theory<sup>1</sup> in conjunction with measured first order sideband amplitudes and are predicted to be about 1% the magnitude of the first order sidebands, which places them below the sensitivity of our detection system.

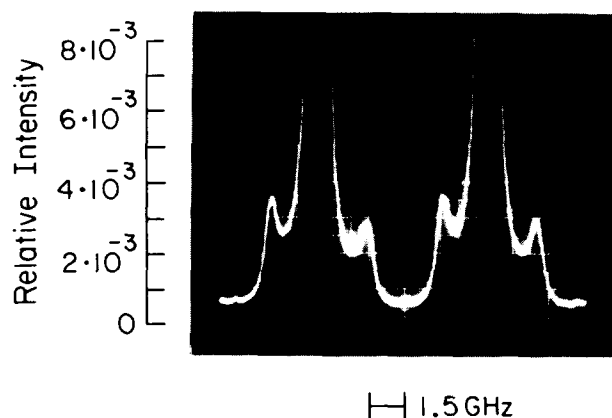


FIG. 1. Fabry-Perot output covering two free-spectral ranges. Vertical scale is normalized to line center.

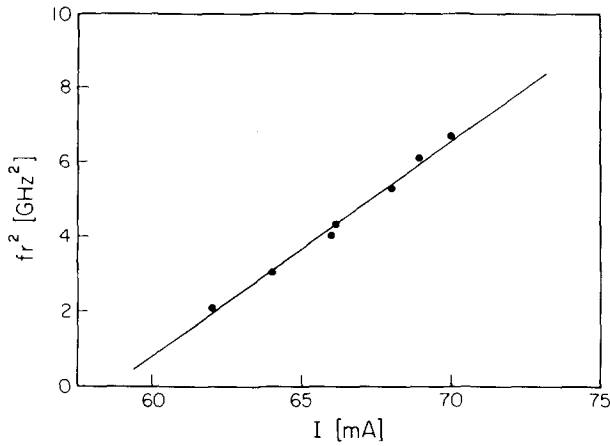


FIG. 2. Square of sideband frequency spacing vs bias current measured for the CSP laser.

It is well known that the square of the relaxation resonant frequency varies linearly with current above threshold.<sup>4</sup> To show that the frequency separation between lasing line center and the first order sidebands is indeed the relaxation resonant frequency we have plotted the square of the measured separation versus current in Fig. 2 for the CSP. It can be seen that the dependence is linear and that the horizontal axis intercept is within experimental error of the threshold current. We observed the same dependence for the BOG. We also observed the resonance in the power fluctuations spectrum using a silicon avalanche photodiode (2.0-GHz bandwidth). Values of the resonant frequency at various bias points were in close agreement with the sideband frequency separation measured in the field spectrum.

Sideband asymmetry was observed at all bias points and always took the form shown in Fig. 1 (i.e., lower frequency sideband larger than the upper sideband). Attempts to misalign the monochromator and the Fabry-Perot resulted in attenuation of the signal, but did not change the form of the asymmetry. We believe this asymmetry results from coher-

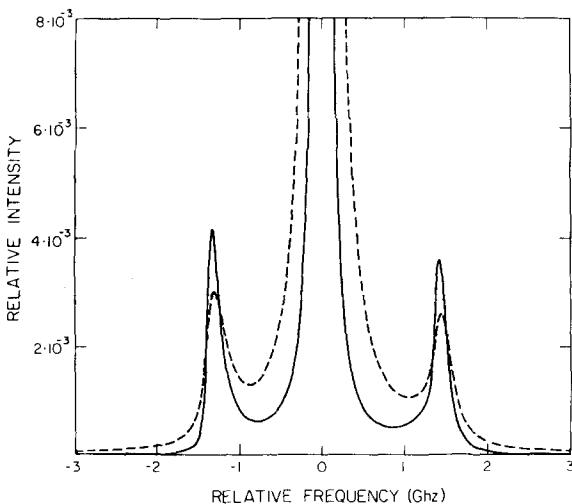


FIG. 3. Solid curve: field spectrum calculated using parameters characteristic of the CSP laser at 2-mW output power per facet. Vertical scale is normalized to line center. Dashed curve: solid curve convolved with instrumental bandwidth Lorentzian.

ence between amplitude and phase fluctuations. Since carrier fluctuations are tied to phase fluctuations through the refractive index, all shot noise sources which involve creation (annihilation) of a photon and simultaneous annihilation (creation) of a carrier would lead to coherence between the ensuing phase and amplitude fluctuations. To test this hypothesis we calculated the field spectrum sidebands using the results given in Ref. 1. Since only first order sidebands are present in the lasers measured, approximations valid for small angle modulation are applicable. Fluctuations of the field are separated into perturbations to field amplitude [ $\delta(t)$ ] and field phase [ $\varphi(t)$ ]:

$$E(t) = [A_0 + \delta(t)] \exp\{i[\omega t + \varphi(t)]\}, \quad (1)$$

where  $E(t)$  is the time-dependent amplitude of the lasing mode and  $\omega$  is the lasing frequency. Using the small angle approximation and Eq. (1), the field autocorrelation is given by

$$\begin{aligned} \langle E(t + \tau) E^*(t) \rangle &= \langle [A_0^2 + A_0 \delta(t) + \delta(t + \tau) \delta(t) \\ &\quad + A_0 \delta(t + \tau)] \\ &\quad \times \exp\{i[\varphi(t + \tau) - \varphi(t)]\} \rangle \\ &\approx A_0^2 \{1 - \frac{1}{2} \langle [\varphi(t + \tau) - \varphi(t)]^2 \rangle\} \\ &\quad + i A_0 \langle \delta(t) \varphi(t + \tau) \rangle \\ &\quad - \langle \delta(t + \tau) \varphi(t) \rangle + \langle \delta(t + \tau) \delta(t) \rangle, \quad (2) \end{aligned}$$

where the lasing frequency has been shifted to the origin for convenience. All terms in this expression are stationary<sup>1</sup> so that the Wiener-Khintchine relation can be applied to calculate the field spectrum. The resulting field spectrum must be used with some care, however, as Eq. (2) is approximate. In particular, the low-frequency behavior (e.g., within three linewidths of line center) will deviate grossly from the correct result, since this approximation is not accurate for large  $\tau$  (i.e., low frequencies in the transform space).<sup>1</sup> Our interest is focused far outside this regime, however, allowing us to proceed with the calculation of the normalized field spectrum  $[2|E(\Omega)|^2/A_0^2]$ :

$$\begin{aligned} \frac{2}{A_0^2} |E(\Omega)|^2 &= D(\Omega) + \frac{1}{2\Omega^2} W_{\Delta\omega}(\Omega) + W_\rho(\Omega) \\ &\quad + i[\langle \rho(\Omega) \varphi(\Omega) \rangle - \langle \rho^*(\Omega) \varphi^*(\Omega) \rangle], \quad (3) \end{aligned}$$

where  $D(\Omega)$  is the delta function,  $W_{\Delta\omega}(\Omega)$  is the frequency fluctuations spectrum,  $W_\rho(\Omega)$  is the amplitude fluctuations spectrum,  $\rho = \delta/A_0$  is the normalized amplitude fluctuation, and  $\Omega$  is the frequency relative to the lasing frequency.  $W_{\Delta\omega}(\Omega)$  and  $W_\rho(\Omega)$  are given in Ref. 1 and  $\langle \rho(\Omega) \varphi(\Omega) \rangle$  can be easily calculated using the rate equations which also appear there. The normalized field spectrum given by Eq. (3) is plotted in Fig. 3 as the solid curve. The amplitude has been normalized to line center and parameters characteristic of the CSP at 2-mW output power per facet have been assumed (spontaneous lifetime  $\tau_s = 1$  ns, gain coefficient  $A = 2.5 \times 10^{-6}$  cm<sup>3</sup>/s, confinement factor  $\Gamma = 0.3$ , transparency carrier density  $n_0 = 0.7 \times 10^{18}$  cm<sup>-3</sup>, photon lifetime  $\tau_p = 2.0$  ps, linewidth broadening factor  $\alpha = 6$ ). The theoretical sideband locations relative to line center as well as sideband amplitudes as shown in Fig. 3 agree reasonably well with those measured as shown in Fig. 1. The observed

sideband asymmetry is also correctly predicted by theory. This asymmetry arises from the terms  $\langle \rho(\Omega) \varphi(\Omega) \rangle$  and  $\langle \rho^*(\Omega) \varphi^*(\Omega) \rangle$  in Eq. (3) and thus reflects the degree of correlation between phase and amplitude fluctuations at the resonance. It is interesting to note that under certain circumstances theory predicts that the asymmetry can change sign (i.e., right sideband larger than left sideband). For typical parameters encountered in semiconductor laser systems, however, it appears that such occurrences are unlikely.

Field fluctuations can be divided approximately into a phase contribution and an amplitude contribution.<sup>1</sup> The phase component is dominant at or near the lasing frequency due to damping of the amplitude component by gain saturation. For frequencies near the field spectrum sidebands, however, gain saturation is inoperative. Calculations showed that at these frequencies the phase component and amplitude component contributions are comparable.

Compared to the theoretical sidebands in Fig. 3 the observed sidebands in Fig. 1 are somewhat smeared. We attribute this to the instrumental broadening of the Fabry-Perot. Although its resolution is roughly 70 MHz, the effective resolution in Fig. 1 is drastically reduced, because of the main lobe's presence. To account for this effect we convolved the theoretical sideband spectrum and a lorentzian with full width at half-maximum equal to our instrumental band-

width. The result shown in Fig. 3 as the dashed curve closely resembles the observed field spectrum.

In summary, we have observed the field spectrum sidebands predicted by Vahala and Yariv. The power dependence of their separation from line center is that characteristic of the relaxation resonant frequency. Sideband asymmetry was also observed, with the left (lower frequency) sideband slightly larger than the right sideband. A theoretical calculation of the field spectrum produced results that agreed very well with observations. Sideband asymmetry can be explained to result from correlation between amplitude and phase fluctuations at the resonance.

The authors thank Dr. M. Nakamura of Hitachi Central Research Laboratories for providing the BOG and CSP lasers used in this experiment. This work was supported by the Office of Naval Research and the National Science Foundation.

<sup>1</sup>K. Vahala and A. Yariv, *Semiclassical Theory of Laser Noise: Part Two*, J. Quantum Electron. (in press).

<sup>2</sup>K. Vahala and A. Yariv, *Semiclassical Theory of Laser Noise: Part One*, J. Quantum Electron. (in press).

<sup>3</sup>J. M. Osterwalder, *IEEE J. Quantum Electron.* **QE-18**, 364 (1982).

<sup>4</sup>H. Kressel and J. Butler, *Semiconductor Lasers and Heterojunction LED's* (Academic, New York, 1977), p. 568.

## Photolysis of KI/Xe mixtures at 193 nm: Observation of KXe\* emission

A. M. Schilowitz and J. R. Wiesenfeld

*Department of Chemistry, Cornell University, Baker Laboratory, Ithaca, New York 14853*

(Received 27 September 1982; accepted for publication 8 November 1982)

Photodissociation of KI at 193 nm in the presence of Xe yields excimer emission in the region 410–530 nm. The intensity distribution differs dramatically from that observed following direct pumping,  $K(5^2P) \leftarrow K(4^2S)$ , the green emission being significantly weaker than that reported previously. Also, the rate of  $K(5^2P)$  deactivation upon collision with Xe is quite inefficient,  $k < 10^{-13} \text{ cm}^3 \text{ molecule}^{-1} \text{ s}^{-1}$ . A simple mechanism involving a curve crossing in KXe resulting in efficient quenching of  $K(5^2P)$  to  $K(5^2S)$  is not supported.

PACS numbers: 31.70.Hq, 33.20.Kf, 34.20.Be

The broadening of alkali metal atomic resonance transitions following collisional perturbation by rare gases has long been the subject of active investigation.<sup>1</sup> These studies have resulted in the accurate description of potentials governing the interaction between these species. In the last decade strong emission has been observed<sup>2</sup> from the electronically excited state of MXe which correlates with  $M(n+1)^2S$  to the lowest molecular state which correlates with  $Mn^2S$ . Such a  $\Sigma$ - $\Sigma$  transition, centered at 525 nm, was observed from KXe following the excitation of the  $K(5^2P \leftarrow 4^2S)$  transition with a tunable dye laser operating

at 404 nm.<sup>3,4</sup> Similar results were obtained following excitation of the ground state KXe molecule with the intense 407-nm line of a krypton ion laser.<sup>5</sup> Other KXe excimer emission bands were detected at 412 nm just to the red of the allowed  $K(5^2P \rightarrow 4^2S)$  transition and at 460 nm close to the forbidden  $3^2D \rightarrow 4^2S$  transition.<sup>3,4</sup>

Time-resolved studies of the kinetic behavior of  $K(5^2P)$  and  $KXe(5s\Sigma)$  following pulsed laser excitation of atomic potassium at 404 nm have been carried out.<sup>4</sup> The temporal behavior of both the atomic and molecular emissions suggested that the excimer was formed in a multistep